


Leaf and shoot apical meristem transcriptomes of quinoa (*Chenopodium quinoa* Willd.) in response to photoperiod and plant development

Nathaly Maldonado-Taïpe¹ | Elodie Rey² | Mark Tester² | Christian Jung¹ | Nazgol Emrani¹ 

¹Plant Breeding Institute, Christian-Albrechts-University of Kiel, Kiel, Germany

²Biological and Environmental Sciences and Engineering Division (BESE), King Abdullah University of Science and Technology (KAUST), Thuwal, Saudi Arabia

Correspondence

Nazgol Emrani, Plant Breeding Institute, Christian-Albrechts-University of Kiel, Am Botanischen Garten 1-9, D-24118 Kiel, Germany.

Email: n.emrani@plantbreeding.uni-kiel.de

Present address

Nathaly Maldonado-Taïpe, Biotechnology and Life Sciences Faculty, Universidad Regional Amazónica Ikiam, Ecuador, South America.

Funding information

King Abdullah University of Science and Technology; Stiftung Schleswig-Holsteinische Landschaft

Abstract

Understanding the regulation of flowering time is crucial for adaptation of crops to new environment. In this study, we examined the timing of floral transition and analysed transcriptomes in leaf and shoot apical meristems of photoperiod-sensitive and -insensitive quinoa accessions. Histological analysis showed that floral transition in quinoa initiates 2–3 weeks after sowing. We found four groups of differentially expressed genes in quinoa genome that responded to plant development and floral transition: (i) 222 genes responsive to photoperiod in leaves, (ii) 1812 genes differentially expressed between accessions under long-day conditions in leaves, (iii) 57 genes responding to developmental changes under short-day conditions in leaves and (iv) 911 genes responding to floral transition within the shoot apical meristem. Interestingly, among numerous candidate genes, two putative *FT* orthologs together with other genes (e.g. *SOC1*, *COL*, *AP1*) were previously reported as key regulators of flowering time in other species. Additionally, we used coexpression networks to associate novel transcripts to a putative biological process based on the annotated genes within the same coexpression cluster. The candidate genes in this study would benefit quinoa breeding by identifying and integrating their beneficial haplotypes in crossing programs to develop adapted cultivars to diverse environmental conditions.

KEYWORDS

day length, differentially expressed genes, floral transition, RNA-seq, transcriptomics

1 | INTRODUCTION

The pseudocereal quinoa (*Chenopodium quinoa* Willd.) is an allotetraploid species ($2n = 4x = 36$) with a genome size of 1.45–1.50 Gb that encompasses 44 776 genes (Jarvis et al., 2017). It resulted from a

hybridization event between an A-genome diploid species that most likely originated from a relative of *Chenopodium pallidicaule* and a B-genome diploid species (*Chenopodium suecicum*, *Chenopodium ficifolium* or another related diploid species) (Jarvis et al., 2017; Štorchová et al., 2015). Quinoa originated from the Andean region of South

[Correction added on 6 March 2024, after first online publication: In the Data Availability Statement, the first sentence has been changed in this version.]

This is an open access article under the terms of the [Creative Commons Attribution-NonCommercial-NoDerivs](https://creativecommons.org/licenses/by-nc-nd/4.0/) License, which permits use and distribution in any medium, provided the original work is properly cited, the use is non-commercial and no modifications or adaptations are made.

© 2024 The Authors. *Plant, Cell & Environment* published by John Wiley & Sons Ltd.

America, where it has grown for over 6000 years as a subsistence crop. Quinoa seeds have a high protein content and an exceptional amino acid composition (Granado-Rodríguez et al., 2021; Iqbal et al., 2020). Moreover, quinoa is tolerant against frost, drought and salinity (Kiani-Pouya et al., 2022). Because of these advantages, it has gained substantial attention as a human diet, and breeding and cultivation have been initiated in over 120 countries (Alandia et al., 2020).

The short-day nature of this crop remains an obstacle to its cultivation in temperate regions and high latitudes in Europe, North America and China (Murphy et al., 2018; Patiranage et al., 2021). A better understanding of the genetic mechanisms underlying floral transition, including photoperiodic regulation of flowering time, will help address this problem. Furthermore, breeding programs aiming to adapt quinoa to new environments can benefit from the profound effect of flowering time control on crop adaptation and yield potential (Gaudinier & Blackman, 2020; Patiranage et al., 2022).

Fuller (1949) published the first report on quinoa's response to photoperiod, where short photoperiods induced earlier inflorescence appearance and flowering than long photoperiods. Since then, only a few studies have elaborated on quinoa's genetic mechanisms of flowering time regulation. Golicz et al. (2020) used a computational approach to identify hundreds of putative orthologs of *Arabidopsis thaliana* flowering time genes in quinoa. They found 611 genes with high sequence homology to *A. thaliana* flowering genes, which could be considered putative flowering time regulators in quinoa. In another study, long noncoding RNA (lncRNA) was analyzed under short-day (SD) conditions with a 60 min night-break (NB) (Wu et al., 2021). The authors identified 24 lncRNA involved in flowering time regulation, some of which may interact with *FLOWERING LOCUS T* (*FT*) and *TWIN SISTER of FT* (*TSF*) homologs based on in silico analysis. Moreover, they found that quinoa homologs of *CONSTANS-like* (*COL*), *LATE ELONGATED HYPOCOTYL* (*LHY*), *EARLY FLOWERING 3* (*ELF3*) and *ELONGATED HYPOCOTYL 5* (*HY5*) were downregulated after NB. In contrast, *PHYTOCROME A* (*PHYA*) and *CRYPTOCHROME1* (*CRY1*) homologs were upregulated after NB. Furthermore, the role of *FT* and *COL* homologs in adapting quinoa to different day-length conditions was highlighted by Patiranage et al. (2021). In their study, the haplotypes of 12 putative flowering time genes were analyzed using a set of 276 accessions grown under long-day (LD) and SD conditions. As a result, *CqFT1A*, *CqCOL2B*, *CqCOL4A-1* and *CqCOL5B* were associated with flowering time variation under LD but not under SD conditions. Recently, a transcriptome study of diurnally collected quinoa samples unveiled *CO-like* transcription factors among the diurnally regulated genes sensitive to the switch from LD to SD (Wu et al., 2023).

The regulation of flowering time has also been studied in quinoa-closely-related species. In *Chenopodium rubrum*, *FLOWERING LOCUS T-LIKE 1* (*CrFTL1*) change of expression was associated with experimental conditions which led to flowering, whereas *CrFTL2* was constitutively expressed (Cháb et al., 2008). Moreover, two *CrCOL* genes were downregulated during the light period regardless of the length of the preceding dark period. Likewise, the floral promoter *CrFTL1* was downregulated during the light period

(Drabešová et al., 2014). In another study, using a segregating *Chenopodium ficifolium* F₂ population, sequence variations at an *FTL1* ortholog explained flowering time, plant height and branching. In a recent study, the transcriptome of *C. ficifolium* was studied at four different developmental stages under LD and SD conditions. The authors identified 6096 differentially expressed genes (DEGs) possibly associated with floral induction. The most relevant candidate genes were those responsible for phytohormone metabolism and signaling since enhanced cytokinin content and the stimulation of cytokinin and gibberellic acid signaling pathways correlated with floral induction under short days (Gutierrez-Larruscain et al., 2022).

This study aimed to determine when the shoot apical meristem (SAM) is turned into a floral meristem. Moreover, our objective was to explore, through transcriptomics, the genes that putatively regulate flowering time and photoperiod response in quinoa. We expected those genes to display differential expression profiles between photoperiods and accessions with contrasting life cycle regimes. Accordingly, we analysed the development of the SAM in two accessions differentially responding to day length. Studying leaf and SAM transcriptomes from plants grown under SD and LD conditions resulted in thousands of DEGs. Our study provides new insight into quinoa's flowering time and photoperiod regulation.

2 | MATERIALS AND METHODS

2.1 | Plant material and growth conditions

Two quinoa accessions were investigated in this study, D-12082 from Peru (seed code: 182301) and PI-614886 from Chile (the sequenced quinoa reference genome QQ74 (Jarvis et al., 2017; Rey et al., 2023, seed code: 182283), which differentially flowered under SD and LD conditions as reported by Patiranage et al. (2021). Plants were grown under 2 day-length regimes (LD and SD). One hundred five plants of each accession were grown in 3 × 3 cm 35-multiwell palettes (Hermann Meyer KG, Germany) in a growth chamber under LD conditions (22°C and 16 h light; 900 μmol·m⁻²·s⁻¹, Son-T Agro 400 W, Koninklijke Philips Electronics N.V.). Likewise, 105 plants of each accession were grown under SD conditions (22°C and 8 h light; 900 μmol·m⁻²·s⁻¹).

2.2 | Phenotyping and histological analysis

In each experiment (LD and SD), we phenotyped 10 plants per accession for days to bolting (days until the floral bud is visible) and days to flowering (days until the first flower opens) (Stanschewski et al., 2021). We sampled seven apices per accession and growth conditions weekly until plants reached the bolting stage (Supporting Information S1: Table 1). We used these apices for histological analysis. Apices were fixed in 4.0% FAA (4.0% formaldehyde, 50.0% ethanol and 5.0% acetic acid) overnight. Then, the samples were dehydrated by an ethanol series and embedded in Paraplast (Sigma, P3683) by a standard protocol (Wu & Wagner, 2012). Apices were

sectioned at 8 μm , using a rotatory microtome (Leica RM 2255) and stained with 0.05% toluidine blue.

2.3 | RNA isolation and DNase treatment

Leaves were harvested at ZT-9 (Zeitgeber-time) and SAMs at ZT-9 to ZT-12 from two accessions at different developmental stages under LD and SD conditions (Supporting Information S1: Table 1). Samples were immediately placed in liquid nitrogen. RNA was isolated from 48 leaf and 24 SAM samples using the peqGold Total RNA Kit (PeqLab) protocol. Ten to 14 SAMs were pooled to make one biological replicate. After RNA isolation, we performed a DNase I treatment (Thermo Fisher Scientific Inc.) for 30 min at 37°C on the isolated RNA to eliminate DNA contamination.

2.4 | Sequencing, reads alignment and transcript assembly

Directional mRNA library preparation was carried out by the Poly(A) enrichment method at Novogene Company Limited. Seventy-two cDNA libraries, prepared from the DNase-treated RNA samples (RIN number > 6.9), were sequenced in 2 × 150 bp paired-end (PE) using NovaSeq. 6000 PE150.

We obtained read-count data from the raw reads following the protocol described by Pertea et al. (2016). Briefly, reads from each sample were first mapped to the QQ74-V2 reference genome of *C. quinoa* cv. QQ74 (CoGe Genome ID: id60716) (Rey et al., 2023) with HISAT2 (v.2.1.9) (Kim et al., 2015). Then, novel and known transcripts were assembled for each sample and merged using StringTie (v.2.2.0) (Pertea et al., 2015). The transcriptome was then retrieved from the merged annotation using the gffread function of GFF utilities (v.0.11.1) (<http://github.com/gpertea/gffcompare>) (Pertea & Pertea, 2020). Next, we obtained the read counts by mapping reads back to the transcripts using bowtie2 (v.2.3.5) (Langmead & Salzberg, 2012) leveraged by rsem (v.1.3.1) (Li & Dewey, 2011) with 'very_sensitive' stringency level. Finally, we extracted the 'expected counts' from each sample to build the gene matrix containing known and novel transcripts. We termed sequences as 'novel transcripts' when they were assembled as transcripts by StringTie (v.2.2.0) but were not annotated in the reference genome. The described pipeline was implemented to address the polyploidy component in the method in our transcriptome analysis, ensuring both stringent read mapping and accurate read counting.

2.5 | Differential expression analysis

The differential expression analysis was carried out at the gene level using R (version 4.1.1) package edgeR (version 3.36.0) (Chen, McCarthy, et al., 2020) as follows. First, we excluded lowly expressed genes by keeping genes with about five read counts or more in a minimum number of samples, where the number of samples is chosen according

to the minimum group sample size. This filtering uses counts per million (CPM) values rather than read counts to avoid giving preference to samples with large library sizes. Later, we normalized the gene expression by the 'trimmed mean of *M* values normalization method' (TMM) (Robinson & Oshlack, 2010), which estimates scale factors between samples, to take library composition into account; thus, obtaining TMM normalized CPM. To view detailed gene expression trends among samples, the Trimmed Mean log ratios (\log_2 fold change of *M* values) (Robinson & Oshlack, 2010) were used for multidimensional scaling (MDS) plots. Next, we used the dgeFitGLM function to fit a generalized linear model to our count data and conducted gene-wise statistical tests for our contrasts. We defined a DEG as the one with a false discovery rate <0.05 and a \log_2 fold change (FC) ≥ 0.25 or ≤ -0.25 .

We investigated the DEGs in two main analyses. First, we used the DEGs of leaf and SAM transcripts annotated in the reference genome QQ74-V2. We compared accessions, day-length conditions and developmental stages (Figure 1) (dgeFitGLM, edgeR). Second, we used novel transcripts to compare accessions, day-length conditions and developmental stages, as done for the annotated transcripts. Later, those DEGs were used to conduct coexpression analyses, as described in the next section.

2.6 | Coexpression analysis

We used coexpression networks to associate novel transcripts to a putative biological process. For this purpose, we combined the DEGs between accessions, day-length conditions and developmental stages obtained for the novel transcripts with the results from the annotated DEGs (dgeFitGLM, edgeR). Then, we used the R package BioNERO (Almeida-Silva & Venancio, 2022) to perform coexpression analyses in the data set containing annotated and novel DEGs. First, we calculated pairwise Pearson correlation coefficients between gene expression patterns. Then, we assessed the interaction between different genes to construct modules using the Weighted Gene Coexpression Network Analysis (WGCNA) algorithm (signed-hybrid network with default parameters) (scale-free power $\beta = 11$ of threshold 0.8, module merging threshold = 0.8; depth split = 10) (Langfelder & Horvath, 2008). Later, we constructed coexpression networks for each of the modules. Then, we selected the top 10% of novel transcripts with the highest degree and a module membership (MM) > 0.7. A degree is defined as the sum of the connection weights of a gene to all other genes in the module, while MM is the correlation of a gene to its module eigengene (Almeida-Silva & Venancio, 2022). As a last step, we blasted the selected novel transcripts using the NCBI Basic Local Alignment Search Tool (BLAST) service to perform blastx (Taxid: 58023; *E* value: 1.0E-3, number of Blast Hits: 3, word size: 6).

2.7 | Gene Ontology (GO) annotation

We carried out GO annotation of the resulting DEGs for each of our analyses (annotated and novel DEGs). First, we used the NCBI BLAST

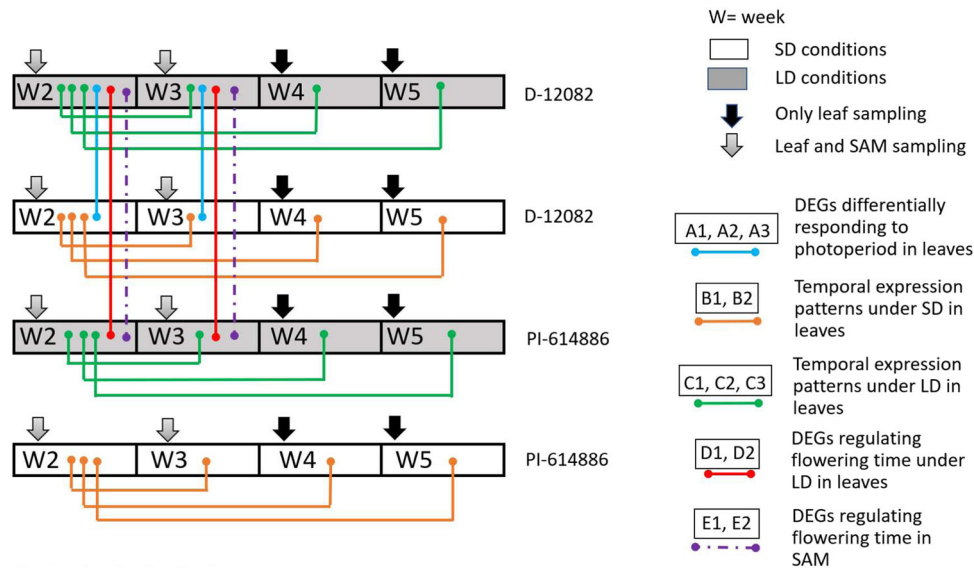


FIGURE 1 Schematic view of the experimental design, sampling points and relevant comparisons between accessions, day-length regimes and developmental stages to identify putative candidate genes. Different comparisons are described using the identifiers in Table 1. Plants were grown in a growth chamber at 22°C under long-day (LD, 16 h light) and short-day conditions (SD, 8 h light). Samples were harvested weekly at ZT-9 (leaves) and ZT-9 to ZT-12 (SAM). SAM, shoot apical meristem; W, week.

service as described above (Taxid: 58023; E value: 1.0E-3, number of Blast Hits: 3, word size: 6). We used the blastx results as input to Blast2GO (version 6.0) to map and annotate GO terms (annotation cut-off: 55, GO-weight: 5) (Gotz et al., 2008). Later, we performed Enzyme Code annotation and Kyoto Encyclopaedia of Genes and Genomes (KEGG) mapping with the Blast2GO tool (Kanehisa & Goto, 2000) using the GENES and PATHWAYS databases (<http://www.genome.ad.jp/kegg/>). When the blastx results of a novel transcript indicated a similarity to a gene previously described in the literature as involved in photoperiod response or flowering time regulation, we investigated the domains of the translated protein in silico (<https://www.ncbi.nlm.nih.gov/Structure/cdd/wrpsb.cgi>).

2.8 | Real-time quantitative polymerase chain reaction (RT-qPCR)

DNase-treated RNA was reverse-transcribed with the First Strand cDNA Synthesis Kit (Thermo Fisher Scientific Inc.), according to the manufacturer's instructions. We performed RT-qPCR by Bio-Rad CFX96 Real-Time System, which has a built-in Bio-Rad C1000 Thermal Cycler (Bio-Rad Laboratories GmbH). We used 18 µL of master mix and 2 µL of diluted (1:20) cDNA per reaction. The master mix composition was as follows: 10 µL of Platinum SYBR Green qPCR SuperMix-UDG with ROX (Invitrogen by Life Technologies GmbH), 1 µL of forward primer, 1 µL of reverse primer and 6 µL of ddH₂O. The amplification conditions were as follows: 95°C for 3 min as initial denaturation and 40 cycles of 10 s at 95°C, 20 s at primer pair annealing temperature and 30 s at 72°C. We amplified three technical replicates per cDNA sample and used water as a template

for negative control reactions. Cq values were obtained by setting the baseline threshold to 100 relative fluorescence units (RFU), and expression levels were calculated by the comparative $\Delta\Delta C_t$ method (Livak & Schmittgen, 2001). Primers used for gene expression analysis are listed in Supporting Information S1: Table 2. *CqPTB* and *CqIDH-A*, identified in our previous study as suitable reference genes for RT-qPCR analysis in quinoa, were used as reference genes (Maldonado-Taibe et al., 2021).

2.9 | Statistical analyses

Pearson's *r* correlation was calculated using MS Excel between the expression values obtained by RNA-seq (dgeFitGLM data contrasts) and those obtained by RT-qPCR ($\Delta\Delta C_t$ method). DTB and DTF significant differences between photoperiod regimes were determined by *t* tests ($\alpha = 0.05$). The correlation between DTF and DTB was calculated and reported as Pearson's correlation coefficient (*r*).

3 | RESULTS

3.1 | Histological investigation of the quinoa shoot apical meristem

Considering the flowering time as 'first flower opens', the accession PI-614886 flowered much earlier than D-12082 under both SD (7 days earlier) and LD (18 days earlier) conditions, as expected from a previous study (Patiranage et al., 2021) (Table 1). However, both accessions bolted simultaneously under SD conditions, while

TABLE 1 Macroscopic and microscopic observations on floral transition in two quinoa accessions.

Accession	Photoperiod	Floral bud appearance		First flower opens		Floral transition based on SAM morphology	
		das ± SD	BBCH	das ± SD	BBCH	das	BBCH
D-12082	LD	46 ± 2 ^a	51	74 ± 3 ^a	60	28	12
	SD	36 ± 2 ^b		56 ± 3 ^b		21	11
PI-614886	LD	31 ± 3 ^a		46 ± 3 ^a		21	
	SD	34 ± 2 ^b		49 ± 3 ^a		21	

Note: D-12082 is a short-day accession from Peru, and PI-614886 is a day-neutral accession from Chile. Plants of each accession were grown in a growth chamber at 22°C under long-day (LD, 16 h light) and short-day conditions (SD, 8 h light). Biologische Bundesanstalt, Bundessortenamt und Chemische Industrie (BBCH) according to Sosa-Zuniga et al. (2017). Lowercase letters show significant differences between photoperiod regimes within accessions determined by *t* test ($\alpha = 0.05$).

Abbreviations: das, days after sowing; SAM, shoot apical meristem.

PI-614886 bolted much earlier than D-12082 under LD. Nevertheless, the opening of the first flower was highly correlated with bolting time in both accessions under LD ($r = 0.57$ and $r = 0.75$) and SD ($r = 0.89$ and $r = 0.47$). Interestingly, D-12082 plants generally showed more vegetative growth (bigger leaves and more branches) under LD than under SD conditions.

We analysed the apices under the microscope to determine when the SAM is turned into a floral meristem under LD and SD in both accessions. We defined the time of floral transition when the SAM exhibited a 'dome shape' phenotype, which corresponds to the SAM morphology at the reproductive stage (apical dominance release) (Dun et al., 2006) (Figure 2). This 'dome shape' was observed when the plants were at a relatively early stage of development, at BBCH11 (first pair of leaves visible) and BBCH12 (second pair of leaves visible) (Sosa-Zuniga et al., 2017) (Supporting Information S2: Figure 1). Under SD conditions, PI-614886 and D-12082 displayed floral transition 3 weeks after sowing whereas, under LD, PI-614886 and D-12082 exhibited floral transition at different time points, 3 and 4 weeks after sowing, respectively (Table 1).

3.2 | Transcriptome sequencing

We sequenced 48 leaf and 24 SAM cDNA libraries from plants grown under SD and LD conditions. In total, 73.37 million reads per library were generated with an average read length of 150 bp, amounting to an average of 11 Gbp per library (Supporting Information S1: Table 3). The average overall mapping rates of the RNA-seq samples of D-12082 (95.79%) and PI-614886 (96.55%) against the reference genome QQ74_V2 differed by less than 1%, which showed that there is no significant read mapping bias between the two accessions at the gene level (Supporting Information S1: Table 3). Moreover, 88.58% and 89.76%, of D-12082 and PI-614886 reads, respectively, aligned uniquely to the genome, showing that the mapping criteria were stringent enough to enable specific mapping between homoeologous copies of genes between quinoa subgenomes. The genome-guided

transcripts assembly produced 132 965 gene models, of which, after excluding the unexpressed genes (those with about five read counts or more in a minimum number of samples), 85 634 gene models in leaf and 74 640 gene models in SAM were retained. A total of 71 230 genes were present in both SAM and leaf tissues. Of the remaining gene models, 26 782 were annotated in the reference genome QQ74-V2 (Rey et al., 2023) and 57 342 were novel transcripts.

We constructed MDS plots with the filtered and normalized leaf and SAM transcriptomes. Following our expectations, we observed that the samples of the same biological replicates corresponding to the same tissue/treatment clustered together (Supporting Information S2: Figure 2). Dimension 1 explained the most variation (19.0%) separating the SAM samples from the leaf samples. Dimension 2 separated the PI-618886 and D-12082 samples and explained 13.0% of the variation (Supporting Information S2: Figure 2).

3.3 | Identification of differentially expressed genes with a putative function as flowering time regulators

First, we analysed the transcripts annotated in the reference genome QQ74-V2. We aimed to identify gene expression profiles that could correlate to the meristem morphological changes. We focused on BBCH11 and BBCH12 (Week 2 [W2] and Week 3 [W3], respectively) developmental stages because our study of the SAM at the histological level showed that floral transition occurred at those stages. We analysed our transcriptome data in four steps. First, we looked for genes differentially responding to photoperiod that putatively regulate flowering time in leaves. Second, we looked for genes that might regulate flowering time under LD conditions in leaves. Third, we searched for genes that may regulate flowering time under SD conditions in leaves. Finally, we screened for the DEGs in SAM to identify flowering time candidate genes in this tissue.

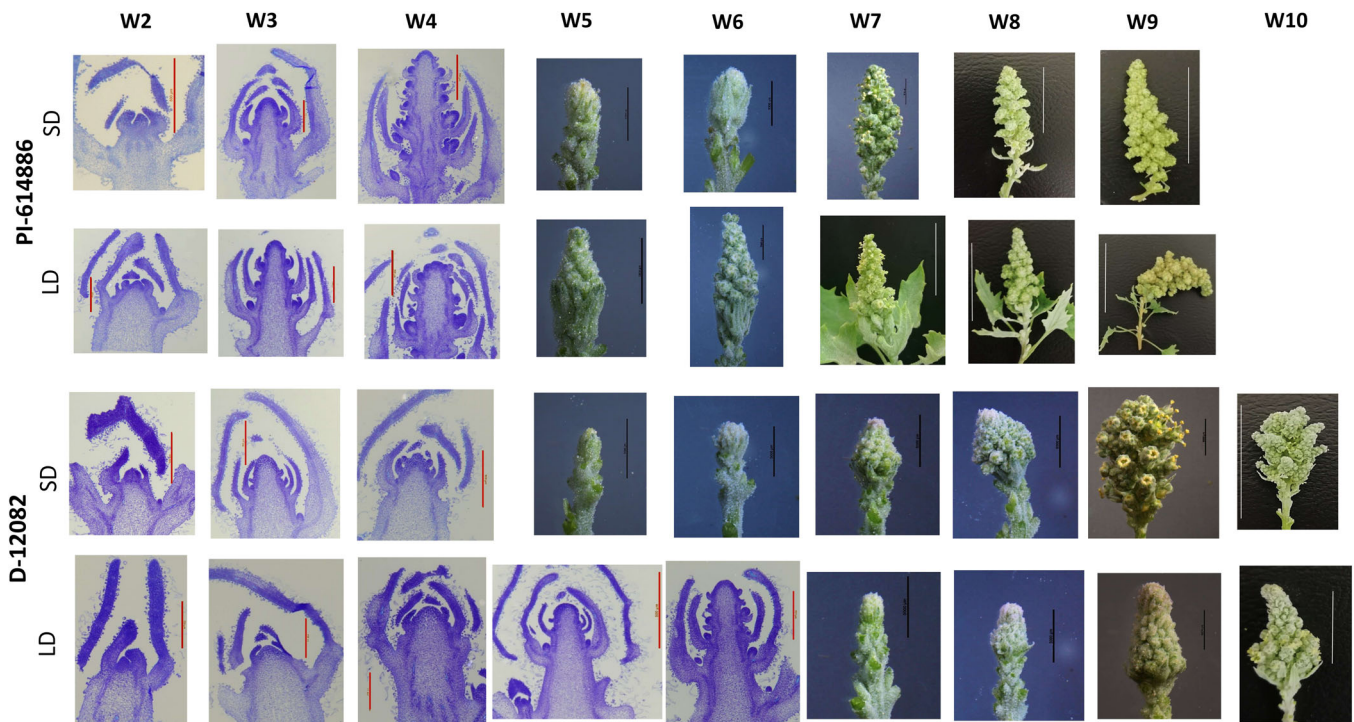


FIGURE 2 Shoot apical meristem (SAM) and inflorescence development from two quinoa genotypes. PI-614886 and D-12082 are day-neutral and short-day accessions, respectively. The SAM longitudinal sections were stained with toluidine blue (Wu & Wagner, 2012). Plants were grown in a growth chamber at 22°C under long-day conditions (LD, 16 h light) and short-day conditions (SD, 8 h light). Photos were taken 2–10 weeks after sowing (W2–W10). A vegetative SAM was identified by an ‘edged’ shape (e.g. W2 accession D-12082, LD), whereas a reproductive meristem was identified by a ‘dome shape’ (e.g. W4 accession D-12082, LD). Scale bars: 500 μm (red), 5000 μm (black) and 37.5 mm (white). [Color figure can be viewed at wileyonlinelibrary.com]

3.3.1 | DEGs responding to photoperiod in leaves

To discover genes differentially responding to photoperiod, we investigated the DEGs between SD and LD conditions at W2 and W3 in D-12082 (solid blue lines in Figure 1) because the morphological changes at the SAM indicated that transition to a floral meristem in this accession occurs in a photoperiod-dependent manner (Supporting Information S2: Figure 3a). We selected the genes for which the expression changes between SD and LD in W2 were significantly different compared to those in W3, given the substantial morphological differences of SAMs between W2 and W3 (accession D-12082). For this purpose, we used the criteria $-0.25 \geq (\log_2 \text{FC at W2} - \log_2 \text{FC at W3}) \geq 0.25$ (Table 2 and Supporting Information S2: Figure 3b).

Subsequently, we investigated the temporal expression pattern of the selected DEGs throughout the plant's development in both accessions under LD and SD (green solid lines and orange solid lines in Figure 1, respectively) (Supporting Information S2: Figure 3c,d). Based on the morphological changes of the SAM, we expected that flowering time genes differentially responding to photoperiod show different temporal expression patterns between SD and LD in the photoperiod-sensitive accession, D-12082, but not in the day-neutral accession, PI-618886. Therefore, we subtracted the DEGs in the day-neutral accession from those in the short-day accession (Supporting Information S2: Figure 3e). Finally, we selected those DEGs that

resulted from the subtraction and were also differentially expressed between LD and SD in D-12082 (solid blue lines in Figure 1 and Supporting Information S2: Figure 3b). As a result, we selected 222 genes differentially responding to photoperiod, which putatively control flowering time in leaves (Table 2 and Figure 3). Among the resulting DEGs and based on a literature survey, we found several genes with a known function in photoperiodic regulation of flowering time in other species like *TREHALOSE-PHOSPHATASE/SYNTHASE 9* (*CqTPS9*), *PHYTOCHROME B* (*CqPHYB*), *ZEITLUPE* (*CqZTL*) and *BLUE-LIGHT INHIBITOR OF CRYPTOCHROMES* (*CqBIC1*) (Figure 3 and Supporting Information S1: Table 4) (Blázquez & Weigel, 1999; Más et al., 2003; Tian et al., 2021; Wang et al., 2016).

3.3.2 | DEGs that putatively regulate flowering time under LD in leaves

As a next step, we searched for genes expressed in the leaves, which putatively regulate flowering time under LD conditions (red solid lines in Figure 1) since we considered the possibility of different flowering time regulators under SD and LD conditions. These genes could be downstream targets of the DEGs differentially responding to photoperiod. We assumed that the main flowering time integrators are the same for the day-neutral and the short-day accessions,

TABLE 2 Summary of differentially expressed genes (DEGs) found by transcriptome sequencing.

Accession	Photoperiod regime	Weeks after sowing (W)	Tissue	Comparison	Identifier	Number of DEGs
D-12082	SD and LD	W2, W3	Leaf	SD versus LD	A1	3769
D-12082	–	–	Leaf	DEGs in comparison A1 ^a	A2	1799
PI-614886	SD	W2, W3, W4, W5	Leaf	W5 versus W4 W5 versus W3 W5 versus W2	B1	3069
PI-614886	LD	W2, W3, W4, W5	Leaf	W5 versus W4 W5 versus W3 W5 versus W2	C1	
D-12082	SD	W2, W3, W4, W5	Leaf	W5 versus W4 W5 versus W3 W5 versus W2	B2	2439
D-12082	LD	W2, W3, W4, W5	Leaf	W5 versus W4 W5 versus W3 W5 versus W2	C2	
D-12082	LD	W2, W3, W4, W5	Leaf	C1 subtracted from C2 (C2–C1)	–	1527
D-12082	–	W2, W3	Leaf	Intersection between (C2–C1) and A2	A3	222 ^b
PI-614886 and D-12082	LD	W2, W3	Leaf	PI-614886 versus D-12082	D1	2687
PI-614886 and D-12082	LD	W2, W3	Leaf	DEGs in comparison D1 ^c	D2	1812 ^b
PI-614886 and D-12082	SD	W2, W3, W4, W5	Leaf	Intersection between C1 and C2	C3	57 ^b
PI-614886 and D-12082	LD	W2, W3	SAM	PI-614886 versus D-12082	E1	1011
PI-614886 and D-12082	LD	W2, W3	SAM	DEGs in comparison E1 ^d	E2	911 ^b

Note: RNA was taken from plants grown in a growth chamber under SD and LD conditions. The comparisons are illustrated in Figure 1.

Abbreviations: FC, fold change; LD, long day; SD, short day; W, week.

^aDEGs were selected based on $-0.25 \geq (\log_2 \text{FC at W2} - \log_2 \text{FC at W3}) \geq 0.25$, where FC = SD/LD.

^bDEGs shown in Figure 3.

^cDEGs were selected based on $-0.25 \geq (\log_2 \text{FC W2} - \log_2 \text{FC W3}) \geq 0.25$, where FC = PI-614886/D-12082.

^dDEGs were selected based on $-0.25 \geq (\log_2 \text{FC}_{\text{acc}} \text{ at W2} - \log_2 \text{FC}_{\text{acc}} \text{ at W3}) \geq 0.25$, where FC = PI-614886/D-12082.

implying that a gene integrating flowering signals would not be accession-dependent. Accordingly, we investigated the DEGs between PI-614886 and D-12082 under LD at W2 and W3 (red solid lines in Figure 1 and Supporting Information S2: Figure 4). From the obtained DEGs, we kept genes with $-0.25 \geq (\log_2 \text{FC W2} - \log_2 \text{FC W3}) \geq 0.25$, whose expression pattern was significantly changed between W2 and W3. The obtained down- and upregulated genes at long-day conditions at Week 2 (referred to as LD.W2 in Figure 3) could serve as putative flowering repressors and promoters, respectively (Figure 4 and Table 2). Among the obtained 1812 DEGs, we found several genes previously reported as flowering time regulators in quinoa and other species (Supporting Information S1: Table 4), for example, *FLOWERING LOCUS T 1* (*CqFT1A*), *FLOWERING LOCUS T 2* (*CqFT2B*), *HEADING DATE 3A* (*CqHD3AB*), *CONSTANS-LIKE 16* (*CqCOL16*), *CONSTANS-LIKE 4* (*CqCOL4*),

FRIGIDA INTERACTING PROTEIN (*CqFIP1*), *FRIGIDA* (*CqFRL4A*) and *EARLY FLOWERING 5* (*CqELF5*) (Choi et al., 2011; Kim et al., 2008; Komiya et al., 2008; Patiranage et al., 2021; Pin et al., 2010; Suárez-López et al., 2001).

3.3.3 | DEGs that putatively regulate flowering time under SD in leaves

In the next step, we searched for genes expressed in leaves that likely regulate flowering time under SD conditions. Since morphological changes at the SAM indicate that both accessions transit to flowering at the same time under SD, we searched for the DEGs in the day-neutral accession with similar temporal expression patterns to those of the short-day accession (orange solid lines in Figure 1). Among the

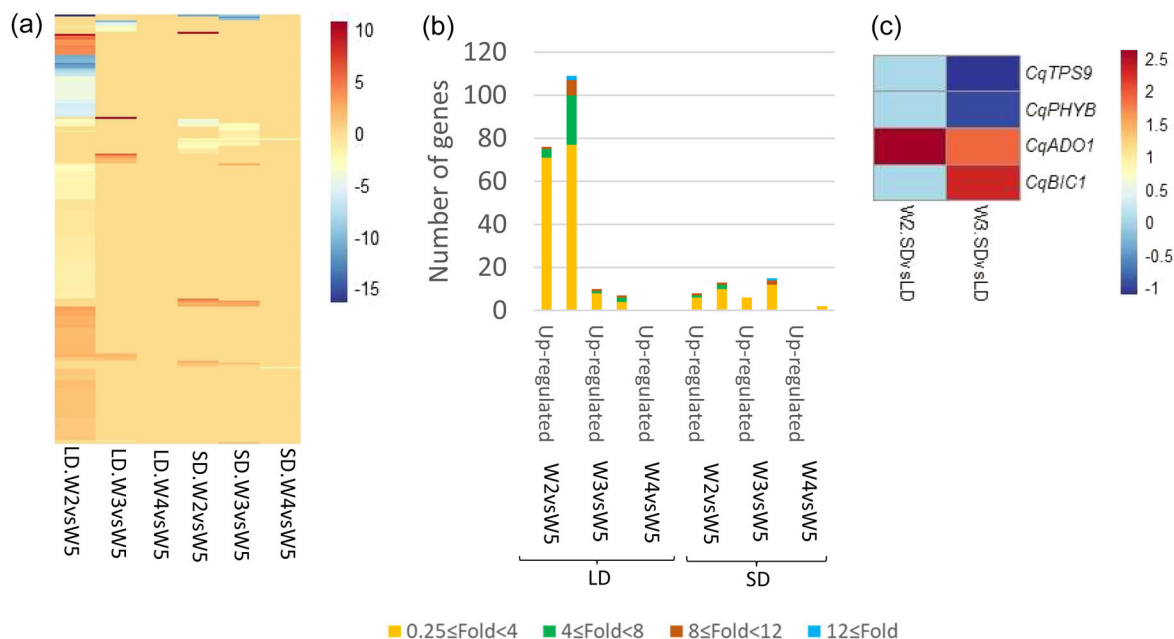


FIGURE 3 DEGs in D-12082 that differentially respond to photoperiod to likely regulate flowering time (identifier A3 in Table 1). (a) Heatmap, (b) number of up- and downregulated genes and (c) selected genes with a known flowering time-related function in other species. Plants were grown under long- and short-day (LD, 16 h light) conditions (SD, 8 h light). RNA was isolated from leaves. LD.W2vsW5 corresponds, for instance, to log₂ (normalized reads in W2/normalized reads in W5). The heatmap was constructed with the pheatmap R package. DEG, differentially expressed genes; W, week. [Color figure can be viewed at [wileyonlinelibrary.com](https://onlinelibrary.wiley.com)]

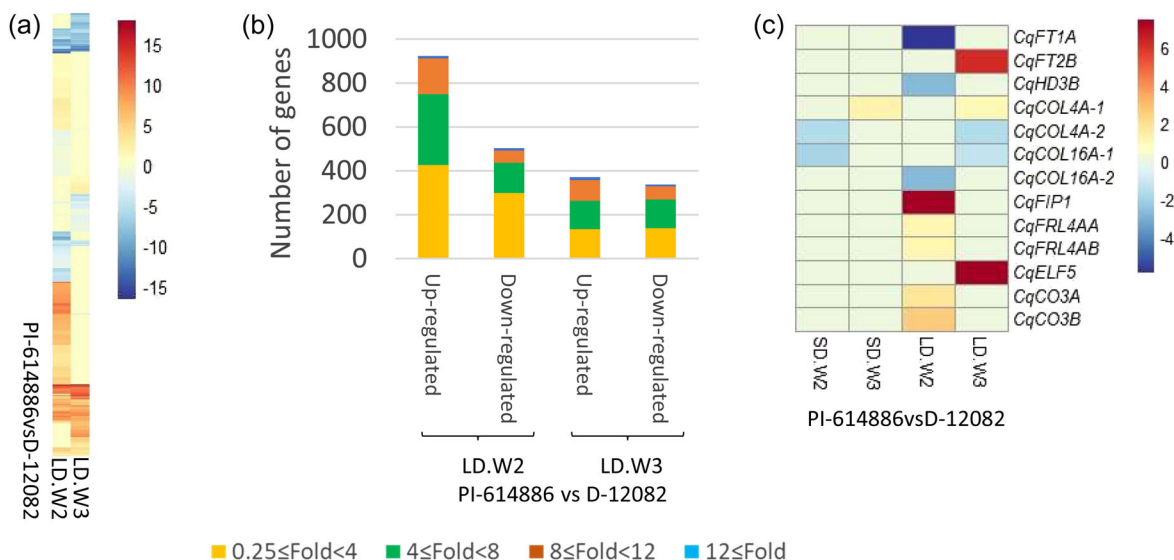


FIGURE 4 DEGs between PI-614886 and D-12082 at W2 and W3 under long-day (LD) conditions putatively control flowering under LD (identifier D2 in Table 1). (a) Heatmap, (b) number of up- and downregulated genes and (c) selected genes with a known flowering time-related function in other species. Plants from the accessions PI-614886 and D-12082 were grown under long-day conditions (LD, 16 h light) and short-day conditions (SD, 8 h light). RNA was isolated from leaves. LD.W2. PI-614886vsD-12082 corresponds, for instance, to log₂ (normalized reads in PI-614886/normalized reads in D-12082). The heatmap was constructed with the pheatmap R package. DEG, differentially expressed genes; W, week. [Color figure can be viewed at [wileyonlinelibrary.com](https://onlinelibrary.wiley.com)]

57 resulting genes, we found *SUPPRESSOR OF CONSTANS OVER-EXPRESSION 1* (*CqSOC1*) (Figure 5 and Supporting Information S1: Table 4), which integrates multiple flowering signals derived from the age-dependent and gibberellin pathways in *Arabidopsis* and other species (Lee & Lee, 2010).

3.3.4 | DEGs that putatively regulate flowering time in SAM

Lastly, we searched for genes putatively regulating flowering time in the SAM. Here, we investigated the DEGs between accessions under

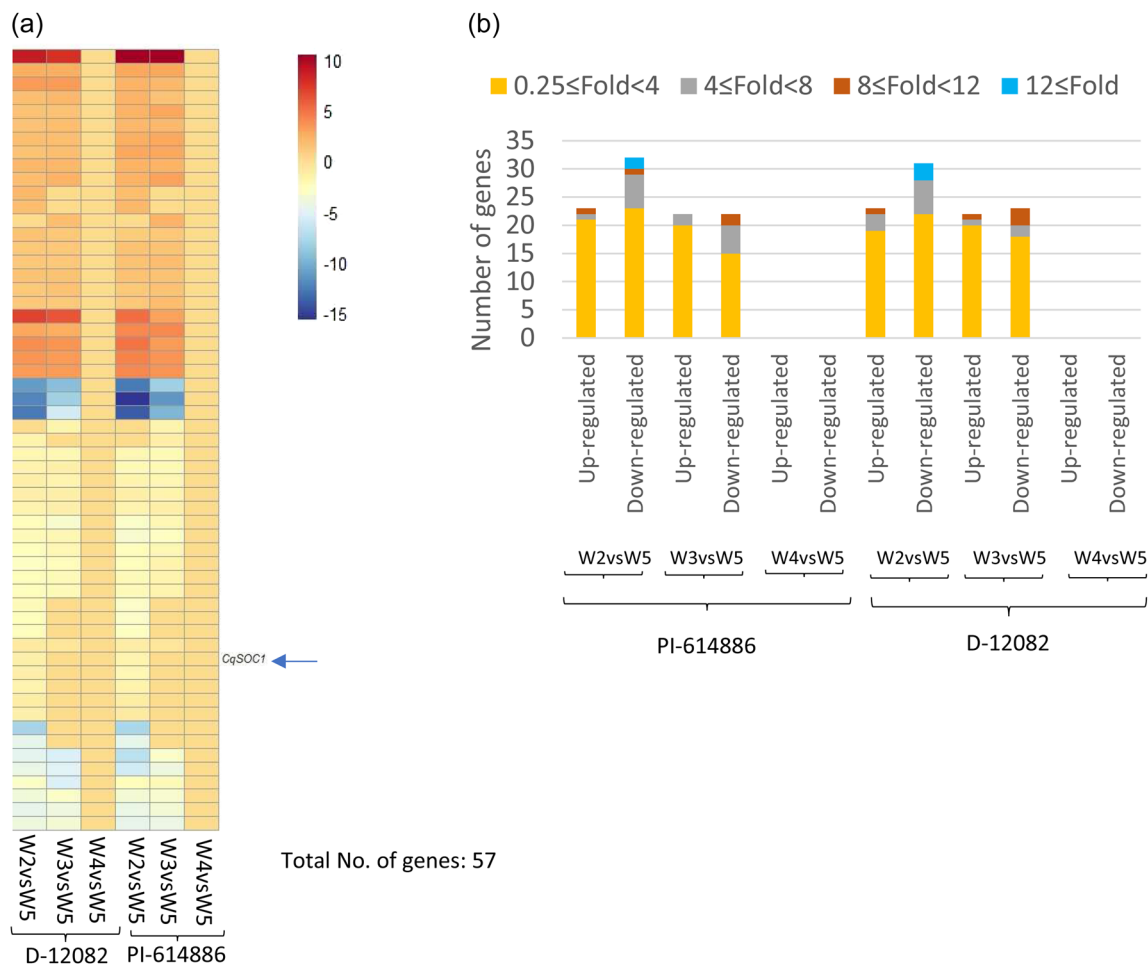


FIGURE 5 DEGs with similar temporal expression patterns in PI-614886 under short-days (SD) putatively control flowering under SD (identifier C3 in Table 1). (a) Heatmap and (b) number of up- and downregulated genes. An arrow shows the expression pattern of SOC1. Plants were grown under long-day conditions and short-day conditions (SD, 8 h light). RNA was isolated from leaves. LD.W2vsW5 corresponds, for instance, to \log_2 (normalized reads in W2/normalized reads in W5). The heatmap was constructed with the pheatmap R package. W, week. [Color figure can be viewed at [wileyonlinelibrary.com](https://onlinelibrary.wiley.com/doi/10.1111/pcpe.14864)]

LD at W2 and W3 when differences in time of floral transition occurred at the SAM (purple dashed lines in Figure 1 and Supporting Information S2: Figure 5). Given the morphological differences observed in the sections of the SAM, the expression fluctuations between the accessions ($\log_2 FC_{acc}$) must be different between W2 and W3 ($-0.25 \geq [\log_2 FC_{acc} \text{ at W2} - \log_2 FC_{acc} \text{ at W3}] \geq 0.25$). In total, 911 DEGs showed differential expression between the accessions under LD conditions but not under SD, where both accessions flowered simultaneously (Figure 6 and Table 2). Interestingly, among these genes, which putatively regulate flowering time in quinoa in the SAM, we found homologs of known flowering time regulators in other species (Supporting Information S1: Table 4). A quinoa homolog of *AGAMOUS-LIKE 15* (*CqAGL15*), a flowering repressor in Arabidopsis (Adamczyk et al., 2007), was downregulated at W2 under LD conditions only in PI-614886 but not in D-12082. A quinoa homolog of *APETALA1* (*CqAP1*), a flowering regulator in Arabidopsis, soybean, wheat and other species (Chen, Nan, et al., 2020; Murai et al., 2003), was upregulated in PI-614886 at W3 under

LD conditions. Moreover, a homolog of *FT INTERACTING PROTEIN 3* (*CqFTIP3*), required to maintain floral meristems in Arabidopsis (Liu et al., 2018), was downregulated at W3 in PI-614886 compared to D-12082.

3.4 | GO of differentially expressed genes

We analysed the putative function of all DEGs identified in this study. The 222 DEGs which differentially respond to photoperiod were mainly allocated to 'Regulation of gene expression' and 'Transcription, DNA-templated' (GO terms: 0010468 and 0006351) under the 'Biological Process' category (Supporting Information S1: Table 5). Furthermore, 56 genes (25.22%) were found in the KEGG database and were allocated to 38 signaling pathways: glycine, serine and threonine metabolism (7.14%), glycolysis/gluconeogenesis (5.36%), among others (Supporting Information S1: Table 6). The percentage of DEGs found in the KEGG database varied from 5.96% to 28.81% when analyzing the DEGs that

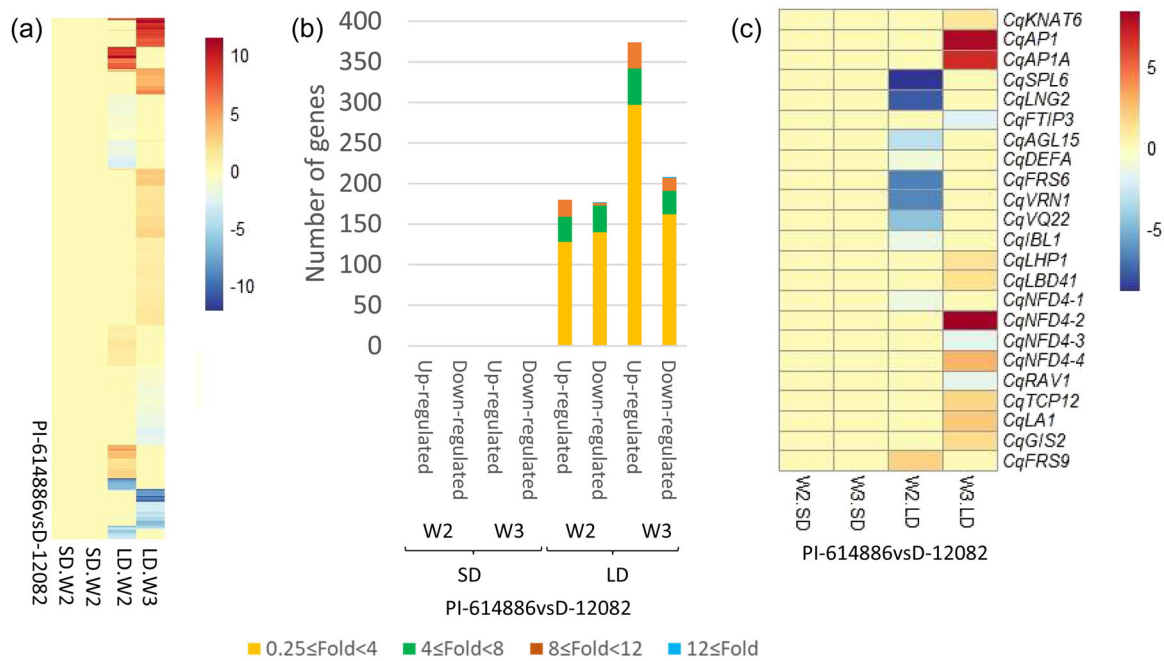


FIGURE 6 DEGs between PI-614886 and D-12082 at W2 and W3 are likely to regulate the time to flower at the shoot apical meristem (SAM) (identifier E2 in Table 1). (a) Heatmap, (b) number of up- and downregulated genes and (c) selected genes with a known flowering time-related function in other species. Plants from the accessions PI-614886 and D-12082 were grown under long-day conditions (LD, 16 h light) and short-day conditions (SD, 8 h light). RNA was isolated from SAM tissue. LD.W2.PI-614886vsD-12082 corresponds, for instance, to log₂ (normalized reads in PI-614886/normalized reads in D-12082). The heatmap was constructed with the pheatmap R package. DEG, differentially expressed genes; W, week. [Color figure can be viewed at [wileyonlinelibrary.com](https://onlinelibrary.wiley.com/doi/10.1111/pcp.14864)]

likely regulate flowering time in the SAM and, under LD and SD conditions, in the leaves (Supporting Information S1: Tables 7–12).

CqCOL16 and *CqELF5*. Furthermore, in Data set 3, the grey module clustered 56 novel DEGs with *CqSOC1*.

3.5 | Coexpression analysis of the DEGs

We performed a coexpression analysis with the novel transcripts and genes annotated in the reference genome QQ74-V2. We hypothesized that genes within the same coexpression cluster might have similar functions. First, we performed a differential expression analysis with the putative novel transcripts as described for the annotated genes (steps described in Table 2 were also carried out for novel transcripts). Second, we grouped the resulting transcripts from the differential expression analysis as follows: novel (89) and annotated (222) DEGs differentially responding to photoperiod (Data set 1); novel (1777) and annotated (1812) DEGs that might regulate flowering time under LD conditions (Data set 2), novel (127) and annotated (57) DEGs that might regulate flowering time under SD conditions (Data set 3) and novel (6229) and annotated (911) DEGs that likely regulate flowering time in the SAM (Data set 4). Third, we performed separate coexpression analyses with these four data sets. As an outcome, we identified six coexpressed modules with Data set 1 (Figure 7). The red module contained the highest number of DEGs (88 DEGs) (Supporting Information S2: Figure 6). Moreover, we identified 20, three and 12 coexpressed modules with Data sets 2, 3 and 4, respectively (Figure 7). The number of DEGs harboured by a module ranged between 72 and 1957 (Supporting Information S2: Figure 6). Interestingly, the grey module of Data set 2 contained 884 novel DEGs with *CqFT1A*, *CqFT2B*,

3.6 | Weighted gene coexpression network analysis

As a next step, we constructed coexpression networks of each module (Supporting Information S2: Figures 7 and 8). We selected 550 novel leaf and 616 SAM transcripts for further examination, representing the top 10% of transcripts in each module with the highest degree and MM > 0.7. We blasted and GO-annotated these novel transcripts to further characterize their putative function (Supporting Information S1: Tables 13 and 14). As an outcome, by BLAST analysis, 84.18% of the novel transcripts in leaves depicted sequence similarity to one or more gene orthologs in other species, out of which 117 (25.27%) coded for uncharacterized proteins. In the case of the SAM tissue, we found that 75.16% of the novel transcripts had sequence similarity to one or more gene orthologs in other species, out of which 177 (38.22%) coded for uncharacterized proteins (Supporting Information S1: Table 13). In total, 148 selected transcripts were annotated to be an isoform of a known gene, and 61 had sequence similarity to genes previously described in the literature as flowering time or photoperiod regulators (Supporting Information S1: Table 15). For instance, we found sequences with similarity to *RICESLEEPER*, whose homologs were associated with days to flowering in quinoa (Maldonado-Taibe et al., 2022) and to *APETALA 2-like* (*AP2*), a flowering time regulator in several species (Debernardi et al., 2020; Shim et al., 2022). We also found sequences with similarity to the

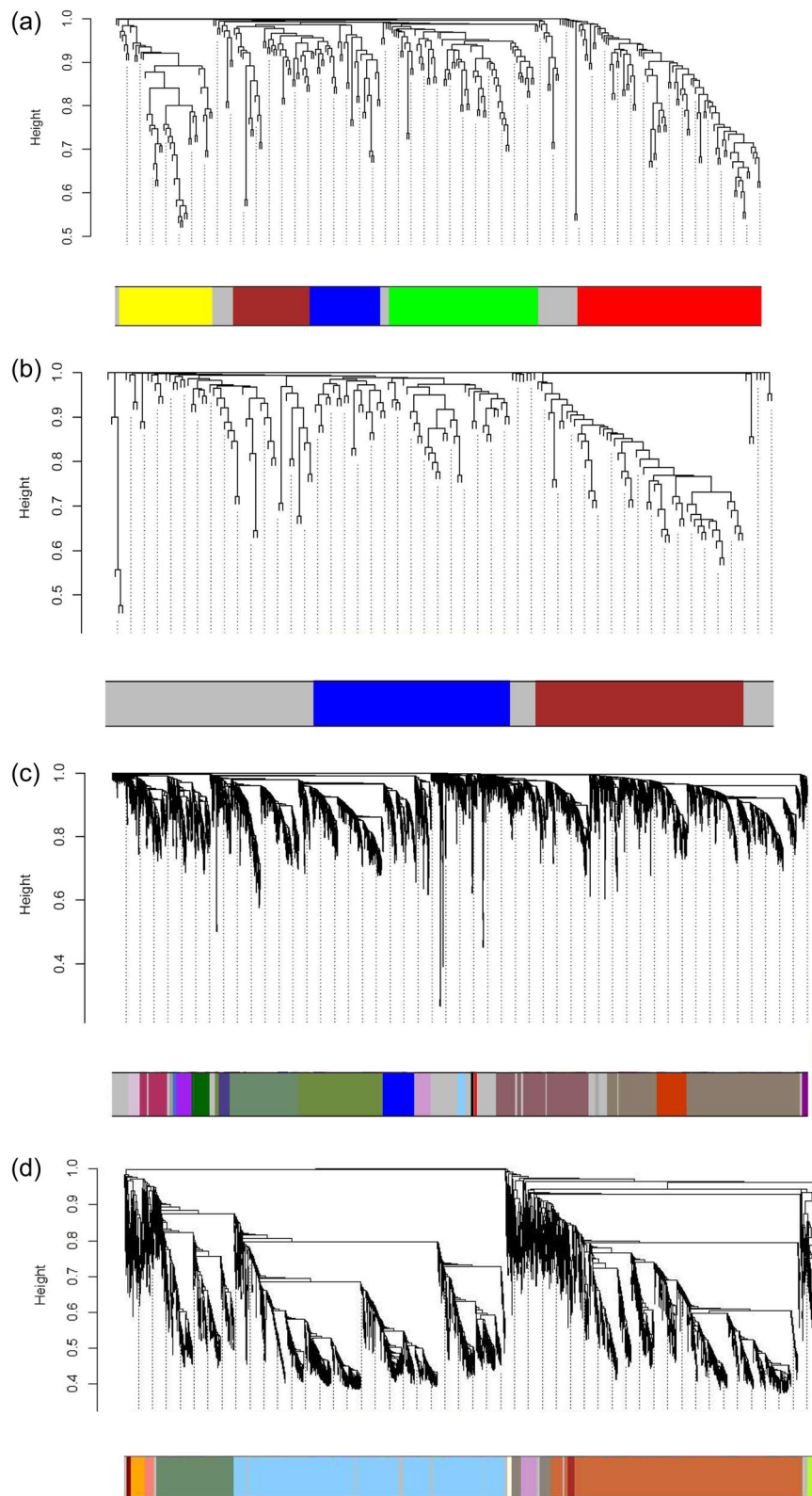


FIGURE 7 Coexpression analysis of annotated and novel (nonannotated) DEGs in leaves. (a) Differentially expressed genes (DEGs) between short-day (SD) and long-day (LD) conditions in D-12082, which differentially respond to photoperiod to likely regulate flowering time (identifier A3 in Table 1 and Figure 1). (b) DEGs between PI-614886 and D-12082 at W2 and W3 under LD are putatively controlling flowering under LD (identifier D2 in Table 1 and Figure 1). (c) DEGs with similar temporal expression patterns between PI-614886 and D-12082 likely control the time to flower under SD (identifier C3 in Table 1 and Figure 1). (d) DEGs between accessions with a putative function of flowering time regulation in the SAM (identifier E2 in Table 1 and Figure 1). Hierarchical clustering dendrograms of the DEGs are shown at the top. Every cluster (module) is shown by a different color at the bottom of the dendrograms. The y-axis (Height) displays the distance between clusters. [Color figure can be viewed at [wileyonlinelibrary.com](https://onlinelibrary.wiley.com)]

Arabidopsis genes *FLOWERING LOCUS M (FLM)*, whose splicing variants are known to repress flowering time (Lutz et al., 2015; Scortecci et al., 2001), and to *ZTL*, which modulates the circadian rhythm (Más et al., 2003).

3.7 | Validation of the RNA-seq results by RT-qPCR

We validated our transcriptome results by performing RT-qPCR analyses with paralogs of *CqTPS9*, *CqZTL*, *CqFIP1*, *CqELF5*, *CqSOC1*, *CqFT2B* and *CqHD3AB* (Supporting Information S1: Table 4). These genes were randomly selected from the list of candidate genes because they are homologs of known flowering time regulators. Then, we calculated the correlation coefficient between the differential expression values from RNA-seq and the $\Delta\Delta C_t$ values from RT-qPCR. The differential expression analyzed by RT-qPCR closely matched the RNA-seq results ($r=0.82$) (Supporting Information S2: Figure 9). Moreover, the expression patterns obtained by RT-qPCR matched our expectations based on our transcriptome data dissection (Figure 8). For instance, *CqZTL* relative expression is higher in D-12082 than in PI-614886 under LD at W3. Thus, *CqZTL* expression is higher in the accession that differentially responds to photoperiod at the stage when flowering commences in LD, based on our histological analysis. These results align with a gene that responds differently to photoperiod to control flowering time. Moreover, the relative expression of *CqZTL* in PI-614886 remains relatively unchanged under both day-length conditions, as expected from PI-614886, a day-neutral accession according to our histological analysis. *CqFT2B* provides another example. This gene's expression was much higher in PI-614886 than in D-12082 under LD at W3, matching our RNA-seq observations (Figure 4). Interestingly, the relative expression of *CqFT2B* was higher towards W3 under SD in both accessions, aligning with the floral transition time as detected in our histological analysis (BBCH11).

4 | DISCUSSION

We present a comprehensive study about the floral transition in quinoa encompassing morphological, phenological and gene expression data. Two accessions with contrasting day-length responses were selected from previous experiments. By histological analysis, we determined when the SAM became a floral meristem. We identified 222 genes differentially responding to photoperiod and 1812 and 57 genes putatively regulating flowering time under LD and SD conditions, respectively. We also identified 911 genes that might regulate flowering time in the SAM.

The histological results placed the floral transition time in quinoa much earlier than the bolting time. We conclude that genes triggering floral transition should be already active at the early stages of quinoa development when the second pair of leaves appears (BBCH12). This agrees with reports in *Chenopodium rubrum*, a species closely related to quinoa, where *CrFTL* genes respond to SD conditions to flower as

early as 5 days after sowing (Cháb et al., 2008). Although floral transition starts early in quinoa, the onset of flowering (when the first flower opens) was recorded several weeks after the floral transition occurred at the SAM, demonstrating that the time to floral transition alone is not the sole predictor of days to flowering. In this case, the time from floral transition until the first flower opens is affected by several environmental factors, as demonstrated in several crops (e.g. tomato, rice, wheat), where nutrient supply, day length, light intensity, light quality and ambient temperature, as well as endogenous signals transmitted by plant hormones play an important role (Bäurle & Dean, 2006; Camejo et al., 2005; Hu et al., 2015).

We searched for genes likely involved in photoperiod response and flowering time regulation based on their differential expression between accessions, day-length conditions and developmental stages. There are constitutively expressed flowering time regulators, such as the *FTL* homolog in *Chrysanthemum* (Higuchi & Hisamatsu, 2015). However, the reason for the experimental design in our study was that many flowering time genes differentially respond to photoperiod, and their expression is correlated with the morphological changes in the SAM (Putterill & Varkonyi-Gasic, 2016). Other possible experimental designs include studying diurnal expression patterns and/or switching between photoperiod regimes. Such experimental settings allowed Wu et al. (2023) to identify *CO-like* transcription factors sensitive to the quinoa switch from LD to SD. Moreover, introducing a night break and studying lncRNA instead of mRNA in quinoa, as done by Wu et al. (2021), would represent another experimental design that would unveil novel candidate genes putatively involved in photoperiod response.

None of the genes found to be down- or upregulated after NB by Wu et al. (2021) (*LHY*, *ELF3*, *HY5*, *PHYA* and *CRY1*) were differentially regulated in our study. However, *CqFT2B* and *CqZTL*, identified by Wu et al. (2023) in a transcriptome study of diurnally collected samples under SD and LD, were also found in our study, which supports their putative role as flowering time regulators. Moreover, Patiranage et al. (2021) obtained comparable findings, indicating that the temporal and diurnal expression of *CqFT2B* in both early- and late-flowering quinoa accessions aligns with the expected expression pattern of a regulator influencing flowering time. Regarding the *CqFT1A* paralog, it has been reported that its expression pattern is not correlated with flowering time (Patiranage et al., 2021; Wu et al., 2023). However, we found that *CqFT1A* would follow the expression profile characteristic of a suppressor of flowering time under LD conditions. The different outcome of our study compared to previous studies might be due to the timing of the sampling, which was at least 1 week earlier than in other studies. This earlier sampling was shown to be beneficial, considering the very early transition of vegetative to reproductive stage in quinoa, identified in this study. Furthermore, Patiranage et al. (2021) found that *CqFT1A* haplotypes in a core collection of 276 quinoa accessions were correlated with early and late flowering time. Under LD conditions, the *CqFT1Aa* haplotype was associated with early flowering, while the *CqFT1Ab* haplotype was correlated with late flowering (Patiranage et al., 2021). Interestingly, the PI-614886 and D-12082 accessions used in our study had the

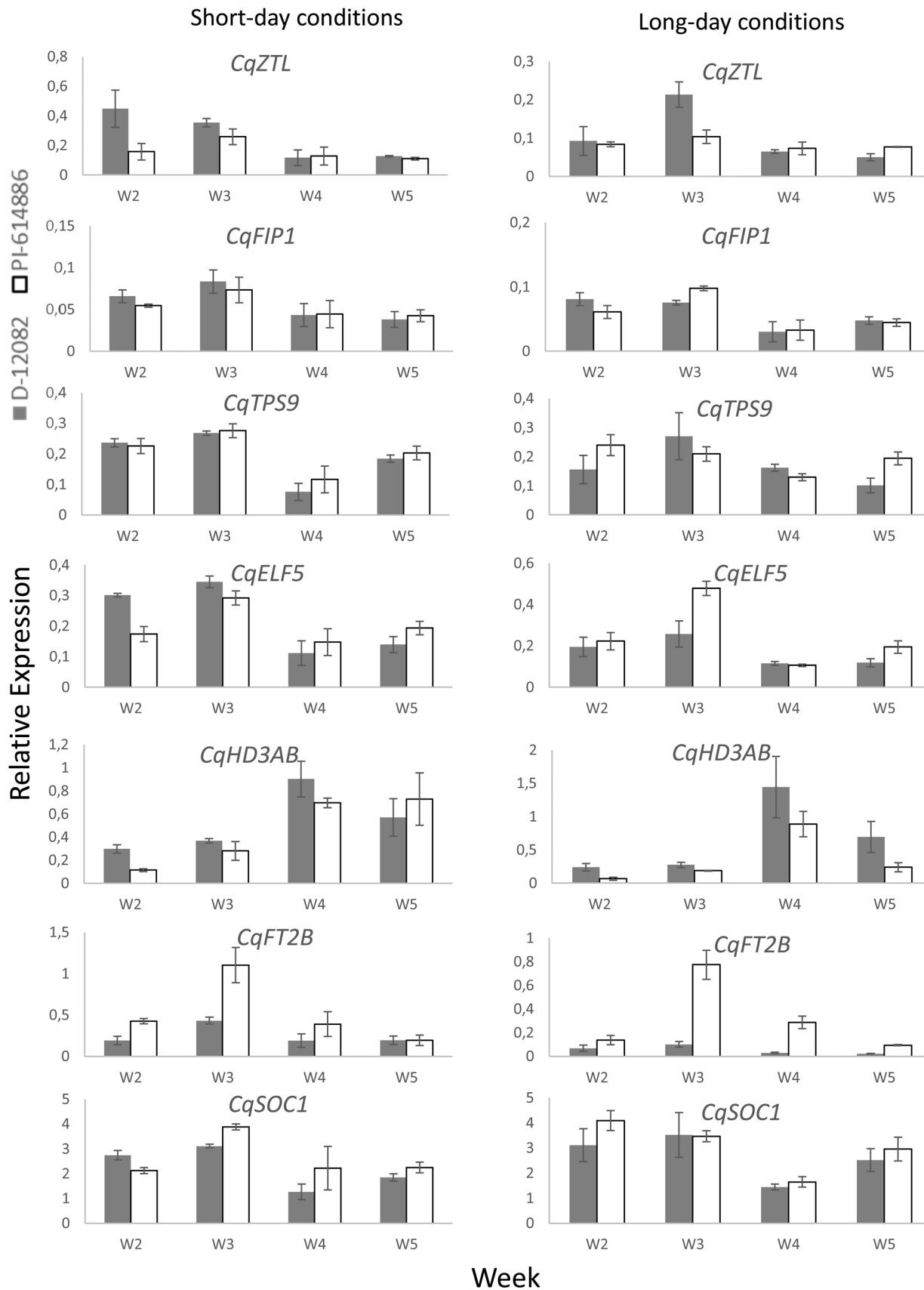


FIGURE 8 Leaf expression profiles of seven genes at different stages of development were obtained by real-time quantitative polymerase chain reaction. Plants from accessions PI-614886 and D-12082 were grown in a growth chamber at 22°C under short-day (SD, 8 h light) and long-day conditions (LD, 16 h light). Three biological replicates and three technical replicates of each biological replicate were used. Error bars: ±standard error of the mean; data were normalized against the geometric mean of *CqPTB* and *CqIDH-A*. W, week.

CqFT1Aa and *CqFT1Ab* haplotypes, respectively. Accordingly, we observed a downregulation of *CqFT1A* at W2 in PI-614886, which flowered earlier than D-12082 under LD, as expected from a floral repressor gene. Noteworthy, the putative function of *CqFT1A* under LD conditions corresponds to *BvFT1* from sugar beet, another member of the *Amaranthaceae* family, where it inhibits flowering under LD. In sugar beet, *BvFT1* has been associated with the transition from vegetative to reproductive growth. Its expression is influenced by environmental cues, such as photoperiod and temperature, suggesting its sensitivity to external signals. *BvFT2* also contributes to flowering time regulation, acting in coordination with *BvFT1* (Pin et al., 2010). Broadly, the role of *FT* genes in plants involves promoting flowering through the encoding of mobile signals that integrate environmental stimuli, especially day length, thereby initiating the shift from vegetative to reproductive growth. In *Arabidopsis thaliana*, *CONSTANS* activates *FT* genes in response to day length, and the interaction of *FT* proteins with genes like *FLOWERING LOCUS D* forms a regulatory network that precisely times flowering in response to environmental cues (Valverde et al., 2004).

The number of differentially expressed genes depends on the experimental design and plant material used, so thousands to tens of thousands of genes will likely change their expression in response to different environments (Sowiński et al., 2020). The number of genes in our study roughly agrees with those in other transcriptome analyses. For instance, comparing four developmental stages of *C. ficifolium* under LD and SD conditions revealed 6096 DEGs (Gutierrez-Larruscain et al., 2022). Moreover, a transcriptome study in quinoa reported 1817 and 8870 genes possibly associated with floral induction under LD and SD, respectively (Gutierrez-Larruscain et al., 2022). A transcriptomic analysis in sugar beet, a member of the *Amaranthaceae* family akin to quinoa, indicated the potential role of numerous genes in responding to vernalization and gibberellic acid (GA) treatment. In that study, the DEGs between the examined conditions varied from 1966 to 4880 (Mutasa-Göttgens et al., 2012).

We hypothesize that most DEGs might be involved in photoperiod-response and flowering time regulation in quinoa. There is increasing evidence that most phenotypes, previously thought to be simply inherited, are controlled by many genes, although with minor effects. The omnigenic paradigm even proposes that any trait is influenced by all genes expressed at a certain time point or developmental stage (Boyle et al., 2017; Mathieson, 2021; Tautz et al., 2020). Examples for complex traits (e.g. floral development, organ size) in maize, sunflower and chilli pepper (Díaz-Valenzuela et al., 2023) have been reported. In a large field study with maize under different environments, 39 and 36 quantitative trait loci (QTL) with minor effects were found for days to silking and days to anthesis, respectively (Buckler et al., 2009). This study showed that differences in flowering time among 5000 inbred lines were not determined by a few genes with large effects but by the minor cumulative effects of numerous QTL. Furthermore, according to the recently proposed omnigenic model, genes can be classified as core or peripheral in their association with a specific trait. Therefore, a

DEG might not belong to flowering-related pathways but play an indirect role, for example, in nutrient uptake or stress response (Cho et al., 2017). Accordingly, we found around 100 DEGs predicted to function as 'Transcription regulator activators' and 'Regulators of gene expression', which are commonly predicted functions for flowering time regulators (Song et al., 2015). However, several other functional categories, not expected to be related to flowering time, were also found, such as 'endopeptidase activity', 'aspartic-type peptidase activity' and 'Udp-glycosyltransferase activity'. Therefore, our results provide further evidence of the omnigenic regulation of flowering time.

Transcriptomics is a powerful tool to identify paralogs that show transcriptional profiles similar to those of a flowering time gene described for other species. Due to quinoa's polyploid nature, we expect neo- or subfunctionalization and gene silencing as in the case of the *PEBP* (*phosphatidyl ethanolamine-binding proteins*) gene family. Out of 24 sequence homologs, only five had been identified as putative *FT* orthologs (Jarvis et al., 2017; Patiranage et al., 2021). Only the leaf transcripts of *CqFT2B* and *CqFT1A* were detected in our study. Furthermore, only one *HD3A*, *SOC1* and *AGL* paralog was identified as a putative flowering time gene based on its expression pattern. Furthermore, our study showed that out of 18 *CONSTANS*-like genes, only *COL16-A1*, *COL16-A2*, *COL4A* and *COL4B* are putative flowering time candidate genes because they showed differential expression between the studied accessions at the time of floral transition (Supporting Information S1: Table 17 and Supporting Information S2: Figure 10).

We found a surprisingly high number of novel transcripts (57 342), including algorithmic artifacts, splice variants and genes that might be specifically transcribed under our experimental conditions. Similar results were reported in a recent study by Zheng et al. (2022), where >50 000 novel transcripts were discovered under cold stress, including splicing variants and 5' or 3' extensions or truncations. Our results are in line with the bioinformatics pipeline used in our investigation, which allows the discovery of putative novel transcripts, isoforms or alternative splicing events. Besides, our bioinformatics pipeline responded to our experimental setting, in which one line used in our study differs from the line used for establishing the reference genome. Therefore, our study yielded more than 6000 genes had not been annotated in the reference genome. Some of these novel transcripts might be line-specific splicing variants. Subsequently, with the coexpression analysis followed by blast and protein domain studies, we could identify promising novel candidate genes based on their association with the annotated candidate genes.

This study provides new insights into floral transition in quinoa by combining morphological and gene expression data. Our study can also broaden the genetic variation utilized in quinoa breeding programs by identifying the beneficial haplotypes of the putative candidate genes and their integration into breeding programs through crosses to develop cultivars adapted to diverse environmental conditions. Differentially expressed genes located within the confidence interval of previously identified flowering time QTL would

be the most promising candidate genes for floral transition in quinoa. Twelve candidate genes from our study had been localized within a major flowering time QTL (Maldonado-Taípe et al., 2022) (Supporting Information S1: Table 16). However, functional characterization is necessary for confirming the role of candidate genes as regulators of flowering time in quinoa. Unfortunately, there is no reliable protocol for quinoa transformation currently. Only a virus-mediated transient expression (VIGS) protocol could enable functional studies in this crop (Ogata et al., 2021).

ACKNOWLEDGEMENTS

The authors thank Bettina Rohardt, Federico Barbier, Monika Bruisch and Florence Muraya for their technical assistance. This study was supported by the Stiftung Schleswig-Holsteinische Landschaft (grant number: 2019/59). The sequencing costs were covered by the baseline funding from King Abdullah University of Science and Technology, Saudi Arabia, to Mark Tester. Open Access funding enabled and organized by Projekt DEAL.

DATA AVAILABILITY STATEMENT

The raw sequencing data of the 72 *C. quinoa* samples sequenced in this study are available on SRA on NCBI under the BioProject PRJNA1070813. Scripts and resources (including the transcripts assembly in fasta format and the matrix of read counts for genes) to perform the bioinformatics and statistical analyses, have been deposited to DRYAD and can be accessed following <https://doi.org/10.5061/dryad.2rnbz7w3>

ORCID

Nazgol Emrani  <http://orcid.org/0000-0001-5673-3957>

REFERENCES

- Adamczyk, B.J., Lehti-Shiu, M.D. & Fernandez, D.E. (2007) The MADS domain factors *AGL15* and *AGL18* act redundantly as repressors of the floral transition in Arabidopsis. *The Plant Journal*, 50(6), 1007–1019.
- Alandia, G., Rodríguez, J.P., Jacobsen, S.-E., Bazile, D. & Condori, B. (2020) Global expansion of quinoa and challenges for the Andean region. *Global Food Security*, 26, 100429.
- Almeida-Silva, F. & Venancio, T.M. (2022) BioNERO: an all-in-one R/ bioconductor package for comprehensive and easy biological network reconstruction. *Functional & Integrative Genomics*, 22(1), 131–136.
- Bäurle, I. & Dean, C. (2006) The timing of developmental transitions in plants. *Cell*, 125(4), 655–664.
- Blázquez, M.A. & Weigel, D. (1999) Independent regulation of flowering by phytochrome B and gibberellins in Arabidopsis. *Plant Physiology*, 120(4), 1025–1032.
- Boyle, E.A., Li, Y.I. & Pritchard, J.K. (2017) An expanded view of complex traits: from polygenic to omnigenic. *Cell*, 169(7), 1177–1186.
- Buckler, E.S., Holland, J.B., Bradbury, P.J., Acharya, C.B., Brown, P.J., Browne, C. et al. (2009) The genetic architecture of maize flowering time. *Science*, 325(5941), 714–718.
- Camejo, D., Rodríguez, P., Angeles Morales, M., Miguel Dell'Amico, J., Torrecillas, A. & Alarcón, J.J. (2005) High temperature effects on photosynthetic activity of two tomato cultivars with different heat susceptibility. *Journal of Plant Physiology*, 162(3), 281–289.
- Cháb, D., Kolář, J., Olson, M.S. & Štorchová, H. (2008) Two *FLOWERING LOCUS T (FT)* homologs in *Chenopodium rubrum* differ in expression patterns. *Planta*, 228(6), 929–940.
- Chen, L., Nan, H., Kong, L., Yue, L., Yang, H., Zhao, Q. et al. (2020) Soybean *AP1* homologs control flowering time and plant height. *Journal of Integrative Plant Biology*, 62(12), 1868–1879.
- Chen, Y., McCarthy, D., Ritchie, M., Robinson, M., Smyth, G. & Hall, E. (2020) edgeR: differential analysis of sequence read count data user's guide. *Bioinformatics*, 26(1), 139–140.
- Cho, L.H., Yoon, J. & An, G. (2017) The control of flowering time by environmental factors. *The Plant Journal*, 90(4), 708–719.
- Choi, K., Kim, J., Hwang, H.-J., Kim, S., Park, C., Kim, S.Y. et al. (2011) The *FRIGIDA* complex activates transcription of *FLC*, a strong flowering repressor in Arabidopsis, by recruiting chromatin modification factors. *The Plant Cell*, 23(1), 289–303.
- Debernardi, J.M., Greenwood, J.R., Jean Finnegan, E., Jernstedt, J. & Dubcovsky, J. (2020) *APETALA 2*-like genes *AP2L2* and *Q* specify lemma identity and axillary floral meristem development in wheat. *The Plant Journal: For Cell and Molecular Biology*, 101(1), 171–187.
- Díaz-Valenzuela, E., Hernández-Ríos, D. & Cibrián-Jaramillo, A. (2023) The role of non-additive gene action on gene expression variation in plant domestication. *EvoDevo*, 14(1), 3.
- Drabešová, J., Cháb, D., Kolář, J., Haškovcová, K. & Štorchová, H. (2014) A dark-light transition triggers expression of the floral promoter *CrFTL1* and downregulates *CONSTANS*-like genes in a short-day plant *Chenopodium rubrum*. *Journal of Experimental Botany*, 65(8), 2137–2146.
- Dun, E.A., Ferguson, B.J. & Beveridge, C.A. (2006) Apical dominance and shoot branching. Divergent opinions or divergent mechanisms? *Plant Physiology*, 142(3), 812–819.
- Fuller, H.J. (1949) Photoperiodic responses of *Chenopodium quinoa* Willd. and *Amaranthus caudatus* L. *American Journal of Botany*, 36, 175–180.
- Gaudinier, A. & Blackman, B.K. (2020) Evolutionary processes from the perspective of flowering time diversity. *New Phytologist*, 225(5), 1883–1898.
- Golicz, A.A., Steinfert, U., Arya, H., Singh, M.B. & Bhalla, P.L. (2020) Analysis of the quinoa genome reveals conservation and divergence of the flowering pathways. *Functional & Integrative Genomics*, 20(2), 245–258.
- Gotz, S., Garcia-Gomez, J.M., Terol, J., Williams, T.D., Nagaraj, S.H., Nueda, M.J. et al. (2008) High-throughput functional annotation and data mining with the Blast2GO suite. *Nucleic Acids Research*, 36(10), 3420–3435.
- Granado-Rodríguez, S., Aparicio, N., Matías, J., Pérez-Romero, L.F., Maestro, I., Gracés, I. et al. (2021) Studying the impact of different field environmental conditions on seed quality of quinoa: the case of three different years changing seed nutritional traits in Southern Europe. *Frontiers in Plant Science*, 12:649132. <https://doi.org/10.3389/fpls.2021.649132>
- Gutierrez-Larruscain, D., Krüger, M., Abeyawardana, O.A.J., Belz, C., Dobrev, P.I., Vaňková, R. et al. (2022) The transcriptomic (RNA-sequencing) datasets collected in the course of floral induction in *Chenopodium ficifolium* 459. *Data in Brief*, 43, 108333.
- Higuchi, Y. & Hisamatsu, T. (2015) *CsTFL1*, a constitutive local repressor of flowering, modulates floral initiation by antagonising florigen complex activity in chrysanthemum. *Plant Science*, 237, 1–7.
- Hu, Y., Liang, W., Yin, C., Yang, X., Ping, B., Li, A. et al. (2015) Interactions of *OsMADS1* with floral homeotic genes in rice flower development. *Molecular Plant*, 8(9), 1366–1384.
- Iqbal, S., Basra, S., Saddiq, M.S., Yang, A., Akhtar, S.S. & Jacobsen, S.-E. (2020) The extraordinary salt tolerance of quinoa. In: Hirich, A., Choukr-Allah, R. & Ragab, R. (Eds.) *Emerging research in alternative crops*. *Environment & Policy*, vol. 58. Cham: Springer, pp. 125–143. https://doi.org/10.1007/978-3-319-90472-6_5

- Jarvis, D.E., Ho, Y.S., Lightfoot, D.J., Schmöckel, S.M., Li, B., Borm, T.J.A. et al. (2017) The genome of *Chenopodium quinoa*. *Nature*, 542(7641), 307–312.
- Kanehisa, M. (2000) KEGG: kyoto encyclopedia of genes and genomes. *Nucleic Acids Research*, 28(1), 27–30.
- Kiani-Pouya, A., Li, L., Rasouli, F., Zhang, Z., Chen, J., Yu, M. et al. (2022) Transcriptome analyses of quinoa leaves revealed critical function of epidermal bladder cells in salt stress acclimation. *Plant Stress*, 3, 100061.
- Kim, D., Langmead, B. & Salzberg, S.L. (2015) HISAT: a fast spliced aligner with low memory requirements. *Nature Methods*, 12(4), 357–360.
- Kim, S.-K., Yun, C.-H., Lee, J.H., Jang, Y.H., Park, H.-Y. & Kim, J.-K. (2008) *OsCO3*, a *CONSTANS-LIKE* gene, controls flowering by negatively regulating the expression of *FT-like* genes under SD conditions in rice. *Planta*, 228(2), 355–365.
- Komiya, R., Ikegami, A., Tamaki, S., Yokoi, S. & Shimamoto, K. (2008) *Hd3a* and *RFT1* are essential for flowering in rice. *Development*, 135(4), 767–774.
- Langfelder, P. & Horvath, S. (2008) WGCNA: an R package for weighted correlation network analysis. *BMC Bioinformatics*, 9(1), 559.
- Langmead, B. & Salzberg, S.L. (2012) Fast gapped-read alignment with Bowtie 2. *Nature Methods*, 9(4), 357–359.
- Lee, J. & Lee, I. (2010) Regulation and function of *SOC1*, a flowering pathway integrator. *Journal of Experimental Botany*, 61(9), 2247–2254.
- Li, B. & Dewey, C.N. (2011) RSEM: accurate transcript quantification from RNA-Seq data with or without a reference genome. *BMC Bioinformatics*, 12, 323.
- Liu, L., Li, C., Song, S., Teo, Z.W.N., Shen, L., Wang, Y. et al. (2018) *FTIP*-dependent *STM* trafficking regulates shoot meristem development in *Arabidopsis*. *Cell Reports*, 23(6), 1879–1890.
- Livak, K.J. & Schmittgen, T.D. (2001) Analysis of relative gene expression data using real-time quantitative PCR and the 2⁻ΔΔCT method. *Methods*, 25(4), 402–408.
- Lutz, U., Posé, D., Pfeifer, M., Gundlach, H., Hagmann, J., Wang, C. et al. (2015) Modulation of ambient temperature-dependent flowering in *Arabidopsis thaliana* by natural variation of *FLOWERING LOCUS M*. *PLoS Genetics*, 11(10), e1005588.
- Maldonado-Taibe, N., Barbier, F., Schmid, K., Jung, C. & Emrani, N. (2022) High-density mapping of quantitative trait loci controlling agronomically important traits in quinoa (*Chenopodium quinoa* Willd.). *Frontiers in Plant Science*, 13, 13.
- Maldonado-Taibe, N., Patirange, D.S.R., Schmöckel, S.M., Jung, C. & Emrani, N. (2021) Validation of suitable genes for normalization of diurnal gene expression studies in *Chenopodium quinoa*. *PLoS one*, 16(3), e0233821.
- Más, P., Kim, W.-Y., Somers, D.E. & Kay, S.A. (2003) Targeted degradation of *TOC1* by *ZTL* modulates circadian function in *Arabidopsis thaliana*. *Nature*, 426(6966), 567–570.
- Mathieson, I. (2021) The omnigenic model and polygenic prediction of complex traits. *The American Journal of Human Genetics*, 108(9), 1558–1563.
- Murai, K., Miyamae, M., Kato, H., Takumi, S. & Ogihara, Y. (2003) *WAP1*, a wheat *APETALA1* homolog, plays a central role in the phase transition from vegetative to reproductive growth. *Plant and Cell Physiology*, 44(12), 1255–1265.
- Murphy, K.M., Matanguihan, J.B., Fuentes, F.F., Gómez-Pando, L.R., Jellen, E.N., Maughan, P.J. et al. (2018) Quinoa breeding and genomics. *Plant Breeding Reviews*, 42, 257–320.
- Mutasa-Göttgens, E.S., Joshi, A., Holmes, H.F., Hedden, P. & Göttgens, B. (2012) A new RNASeq-based reference transcriptome for sugar beet and its application in transcriptome-scale analysis of vernalization and gibberellin responses. *BMC Genomics*, 13, 99.
- Ogata, T., Toyoshima, M., Yamamizo-Oda, C., Kobayashi, Y., Fujii, K., Tanaka, K. et al. (2021) Virus-mediated transient expression techniques enable functional genomics studies and modulations of betalain biosynthesis and plant height in quinoa. *Frontiers in Plant Science*, 12, 12.
- Patirange, D.S., Asare, E., Maldonado-Taibe, N., Rey, E., Emrani, N. & Tester, M. et al. (2021) Haplotype variations of major flowering time genes in quinoa unveil their role in the adaptation to different environmental conditions. *Plant, Cell & Environment*, 44(8), 2565–2579.
- Patirange, D.S., Rey, E., Emrani, N., Wellman, G., Schmid, K., Schmöckel, S.M. et al. (2022) Genome-wide association study in quinoa reveals selection pattern typical for crops with a short breeding history. *eLife*, 11, e66873.
- Pertea, G. & Pertea, M. (2020) GFF utilities: GffRead and GffCompare. *Research; A Journal of Science and its Applications*, 9, 304.
- Pertea, M., Kim, D., Pertea, G.M., Leek, J.T. & Salzberg, S.L. (2016) Transcript-level expression analysis of RNA-seq experiments with HISAT, StringTie and Ballgown. *Nature Protocols*, 11(9), 1650–1667.
- Pertea, M., Pertea, G.M., Antonescu, C.M., Chang, T.-C., Mendell, J.T. & Salzberg, S.L. (2015) StringTie enables improved reconstruction of a transcriptome from RNA-seq reads. *Nature Biotechnology*, 33(3), 290–295.
- Pin, P.A., Benlloch, R., Bonnet, D., Wremerth-Weich, E., Kraft, T., Gielen, J.J.L. et al. (2010) An antagonistic pair of *FT* homologs mediates the control of flowering time in sugar beet. *Science*, 330(6009), 1397–1400.
- Putterill, J. & Varkonyi-Gasic, E. (2016) *FT* and *florigen* long-distance flowering control in plants. *Current Opinion in Plant Biology*, 33, 77–82.
- Rey, E., Maughan, P.J., Maumus, F., Lewis, D., Wilson, L., Fuller, J. et al. (2023) A chromosome-scale assembly of the quinoa genome provides insights into the structure and dynamics of its subgenomes. *Communications Biology*, 6(1), 1263.
- Robinson, M.D. & Oshlack, A. (2010) A scaling normalization method for differential expression analysis of RNA-seq data. *Genome Biology*, 11(3), R25.
- Scortecchi, K.C., Michaels, S.D. & Amasino, R.M. (2001) Identification of a *MADS*-box gene, *FLOWERING LOCUS M*, that represses flowering. *The Plant Journal*, 26(2), 229–236.
- Shim, Y., Lim, C., Seong, G., Choi, Y., Kang, K. & Paek, N.C. (2022) The *AP2/ERF* transcription factor *LATE FLOWERING SEMI-DWARF* suppresses long-day-dependent repression of flowering. *Plant, Cell & Environment*, 45(8), 2446–2459.
- Song, Y.H., Shim, J.S., Kinmonth-Schultz, H.A. & Imaizumi, T. (2015) Photoperiodic flowering: time measurement mechanisms in leaves. *Annual Review of Plant Biology*, 66, 441–464.
- Sosa-Zuniga, V., Brito, V., Fuentes, F. & Steinfurt, U. (2017) Phenological growth stages of quinoa (*Chenopodium quinoa*) based on the BBCH scale. *Annals of Applied Biology*, 171(1), 117–124.
- Sowiński, P., Fronk, J., Jończyk, M., Grzybowski, M., Kowalec, P. & Sobkowiak, A. (2020) Maize response to low temperatures at the gene expression level: a critical survey of transcriptomic studies. *Frontiers in Plant Science*, 11, 576941.
- Stanschewski, C.S., Rey, E., Fiene, G., Craine, E.B., Wellman, G., Melino, V.J. et al. (2021) Quinoa phenotyping methodologies: an international consensus. *Plants*, 10(9), 1759.
- Štorchová, H., Drabešová, J., Cháb, D., Kolář, J. & Jellen, E.N. (2015) The introns in *FLOWERING LOCUS T-LIKE (FTL)* genes are useful markers for tracking paternity in tetraploid *Chenopodium quinoa* Willd. *Genetic Resources and Crop Evolution*, 62, 913–925.
- Suárez-López, P., Wheatley, K., Robson, F., Onouchi, H., Valverde, F. & Coupland, G. (2001) *CONSTANS* mediates between the circadian clock and the control of flowering in *Arabidopsis*. *Nature*, 410(6832), 1116–1120.
- Tautz, D., Reeves, G. & Pallares, L.F. (2020) New experimental support for long standing concepts of polygenic genetics implies that the Mendelian genetic paradigm needs to be revised: the new (old) genetics, version 1.0. *NAL-Live*, 2020(1), 1–15.

- Tian, H., Li, Y., Wang, C., Xu, X., Zhang, Y., Zeb, Q. et al. (2021) Photoperiod-responsive changes in chromatin accessibility in phloem companion and epidermis cells of Arabidopsis leaves. *The Plant Cell*, 33(3), 475–491.
- Valverde, F., Mouradov, A., Soppe, W., Ravenscroft, D., Samach, A. & Coupland, G. (2004) Photoreceptor regulation of *CONSTANS* protein in photoperiodic flowering. *Science (New York, N.Y.)*, 303(5660), 1003–1006.
- Wang, Q., Zuo, Z., Wang, X., Gu, L., Yoshizumi, T., Yang, Z. et al. (2016) Photoactivation and inactivation of Arabidopsis cryptochrome 2. *Science*, 354(6310), 343–347.
- Wu, M.-F. & Wagner, D. (2012) RNA in situ hybridization in Arabidopsis. In: Jin, H. & Gassmann, W. (Eds.) RNA abundance analysis. *Methods in Molecular Biology*, vol. 883. Totowa, NJ: Humana Press, pp. 75–86. https://doi.org/10.1007/978-1-61779-839-9_5
- Wu, Q., Bai, X., Luo, Y., Li, L., Nie, M., Liu, C. et al. (2023) Identification of the global diurnal rhythmic transcripts, transcription factors and time-of-day specific *cis* elements in *Chenopodium quinoa*. *BMC Plant Biology*, 23(1), 96.
- Wu, Q., Luo, Y., Wu, X., Bai, X., Ye, X., Liu, C. et al. (2021) Identification of the specific long-noncoding RNAs involved in night-break mediated flowering retardation in *Chenopodium quinoa*. *BMC Genomics*, 22(1), 284.
- Zheng, L., Zhao, Y., Gan, Y., Li, H., Luo, S., Liu, X. et al. (2022) Full-length transcriptome sequencing reveals the impact of cold stress on alternative splicing in quinoa. *International Journal of Molecular Sciences*, 23(10), 5724.

SUPPORTING INFORMATION

Additional supporting information can be found online in the Supporting Information section at the end of this article.

How to cite this article: Maldonado-Taipe, N., Rey, E., Tester, M., Jung, C. & Emrani, N. (2024) Leaf and shoot apical meristem transcriptomes of quinoa (*Chenopodium quinoa* Willd.) in response to photoperiod and plant development. *Plant, Cell & Environment*, 47, 2027–2043. <https://doi.org/10.1111/pce.14864>